Chinese Chemical Letters 34 (2023) 108179

Contents lists available at ScienceDirect

Chinese Chemical Letters

journal homepage: www.elsevier.com/locate/cclet

Synthesis, structure, and host-guest chemistry of a pair of isomeric selenanthrene-bridged molecular cages ☆

Wanqian Lv[a], Yunyi Song[a], Xinyuan Lv[a], Jun Yuan[b,*], Kelong Zhu[a,*]

[a] School of Chemistry, Sun Yat-sen University, Guangzhou 510275, China
[b] School of Innovation and Entrepreneurship, Shaoguan University, Shaoguan 512005, China

ARTICLE INFO

Article history:
Received 26 November 2022
Revised 15 January 2023
Accepted 29 January 2023
Available online 1 February 2023

Keywords:
Selenanthrene
Crown ether
Molecular cage
Möbius strip
Host-guest chemistry

ABSTRACT

A pair of selenanthrene-bridged molecular cages have been constructed through a one-step cyclization reaction of a tetrakis(iodo) crown ether with selenium powder. The tubular belt-shaped cage has an intrinsic cavity which can adaptively transform to accommodate electron-deficient guests forming [2]pseudorotaxane complexes. The other product was determined to be an isomeric cage featuring a Möbius strip structure, which exhibits slower twist-migration dynamics than its thianthrene counterpart. The success of using selenanthrene as joints enables an alternative way to structural design and property regulation of molecular cages.

Double stranded belt- or strip-shaped macrocycles are attractive to many chemists not only for their intriguing structures, but also potential applications in supramolecular chemistry and material science [1–12]. Owing to their intrinsic deep cavities, the tubular belt-shaped cages have been widely served as molecular containers which could enable absorption and separation [13], controlled release [14,15], and catalysis [16,17]. With the assistance of a conjugate carbon nanobelt, precise construction of nanotubes could also be achieved [18,19]. More interestingly, the double linkages could also produce twists in the cyclic backbones and allow access to molecular Möbius strips which are isomeric to their tubular counterparts [20–23]. The unique topological structure of a molecular Möbius strip could be further useful in fabricating molecular knots [24,25]. Despite recent progresses in the field of molecular belt and cage chemistry, it remains essential and challenging to develop facile synthetic methods for double stranded belt-shaped cages with diverse structures and properties.

Recently, we have reported a series of heteroatom (S or O) embedded molecular belts by taking advantage of utilizing conformationally dynamic hetero-anthracenes as building blocks [26–30]. Noteworthily, the lateral fusion of thianthrene (TA) with dibenzo[24]crown-8 ether (DB24C8) has successfully afforded a pair of isomeric molecular cages featuring a tubular or a Möbius strip-shaped geometry [30]. To further explore the scope of this chemistry, we have now taken diselenin into account as the joint for constructing cage products (Fig. 1). Comparing with TA, selenanthrene (SeA) is generally less explored especially in both synthetic and host-guest chemistry. With the smaller bending angle ($\phi \sim 125°$) and a larger barrier of ring inversion [31,32], fine tuning the molecular geometry and skeleton dynamics would become possible when SeA is employed as the building block. Moreover, the less electronegativity of selenium than sulfur may further induce enhanced binding affinity of a cage towards electron-deficient guest molecules. Although a few of selenium-containing macrocycles have been previously reported [33–35], selenanthrene-bridged molecular cages are still rare and their properties remain largely under explored. Herein, we report the synthesis, structure determination, and host-guest complexation of two unprecedented belt-like molecular cages composed of SeA and DB24C8 moieties.

To build the SeA-bridged cages, we have adopted a facile one-pot cyclization reaction developed previously for constructing the thianthrene counterparts [30]. Accordingly, optimization of the synthetic conditions has been conducted (Table S1 in Supporting information). As depicted in Fig. 2a, directly reacting the readily available tetrakisiodo-DB24C8 (2) with selenium powder in the presence of catalytic amount of cuprous iodide successfully afforded two products **1a** and **1b** with isolated yield of 6% and 2%, respectively. Both products were then subjected to high-resolution mass spectrometry (HR-MS) analysis (Figs. S1 and S2 in Supporting information). The observed isotopic distribution of the predominant signal peak at *m/z* of 1229.0156, corresponding to [**1a**·Na]$^+$, is

☆ Dedication to Prof. Lixin Dai on the Occasion of His Centenary Birthday.

* Corresponding authors.
E-mail addresses: yuanj9@mail2.sysu.edu.cn (J. Yuan), zhukelong@mail.sysu.edu.cn (K. Zhu).

https://doi.org/10.1016/j.cclet.2023.108179
1001-8417/

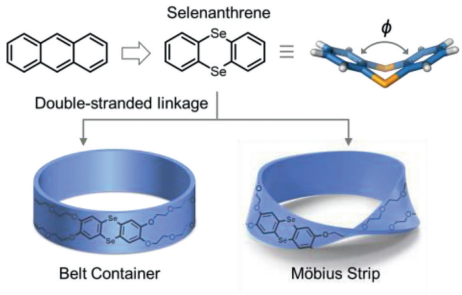

Fig. 1. Schematic representation of a pair of selenanthrene-bridged molecular cages composed of SeA and DB24C8.

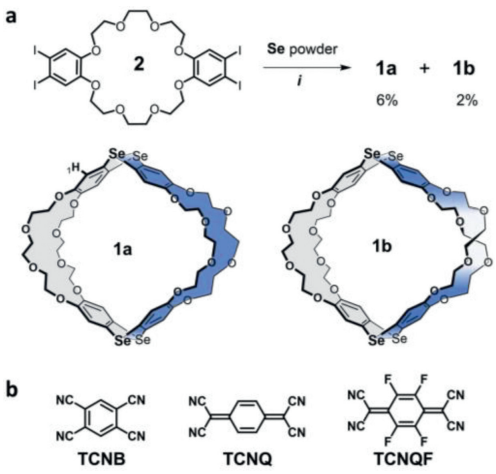

Fig. 2. (a) Synthesis of selenanthrene-bridged cage **1a** and **1b**. Condition *i*: CuI, phenanthroline, K_2CO_3, dimethylacetamide, 150 °C, 72 h. (b) Guest molecules employed in this study.

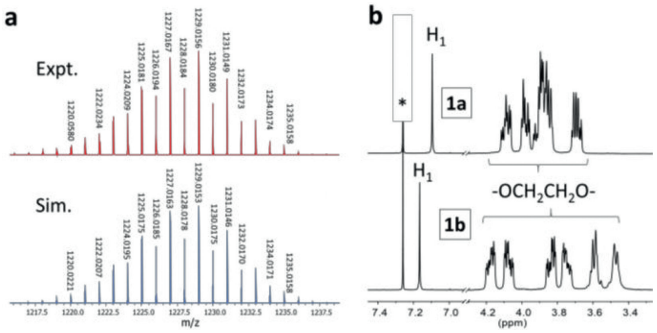

Fig. 3. (a) Experimental (red) and simulated (blue) isotopic distribution for [**1a**·Na]$^+$ on mass spectroscopy; (b) Partial ^{1}H NMR (400 MHz, $CDCl_3$, 298 K) spectra of **1a** (top) and **1b** (bottom). *$CHCl_3$.

in good consistence with simulation confirmed its correct molecular formula as desired (Fig. 3a). The HR-MS analysis of **1b** revealed an identical pattern as that of **1a** indicating a possible isomeric product (Fig. S2). However, both **1a** and **1b** have inferred symmetrical structures based on their proton NMR spectra (Fig. 3b). Only a singlet resonance peak for aromatic protons, at 7.10 and 7.17 ppm for **1a** and **1b** respectively, was observed. The resonance peaks for protons of ethylene glycol ether are similar but distinguishable. Therefore, **1a** and **1b** are most likely either a tubular or a Möbius belt-shaped cage with rapid skeleton dynamics at ambient temperature as that of thianthrene-bridged cages.

The molecular structure of **1a** and **1b** were then unambiguously determined by single crystal X-ray diffraction (SCXRD) measurement (Tables S2 and S3 in Supporting information). **1a** exhibits

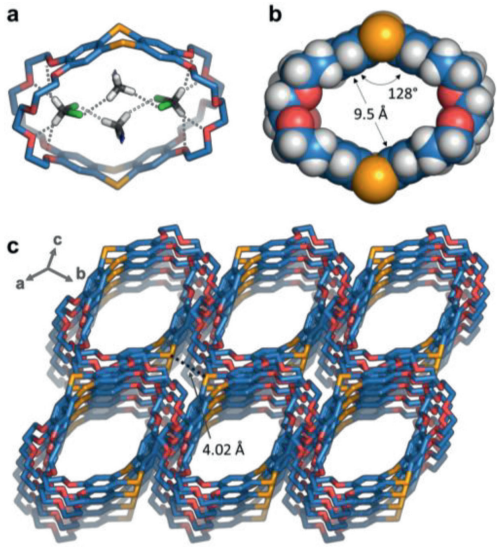

Fig. 4. Crystal structures of **1a**. Hydrogen bonds are highlighted in gray dash lines. Color code: Se = Orange, O = red, N = deep blue, C = light blue and gray, Cl = green, H = white.

a centrosymmetric molecular structure with a well-defined belt shape (Figs. 4a and b). Each crown ether moiety adopts a C-shaped conformation and clamps on a molecule of dichloromethane with assistance of C–H···O hydrogen bondings. The macrocyclic cavity is further filled up by two molecules of acetonitrile forming C–H···Cl hydrogen bondings between dichloromethanes. Such an inflated complex structure renders a bending angle of 128° for the SeA unit which is slightly larger than that of a free SeA [25,26]. The opening cavity gives a separation of *ca.* 9.5 Å between the two parallel benzene rings indicating sufficient room spaces potential for accommodating flat guest molecules *via* π-π stacking interactions. The overall geometry of **1a** are quite similar to that of a thianthrene cage [30]. Interestingly, **1a** stacks along the *c* crystal coordinate axis to yield one-dimensional channels which can further pack and expand into a three-dimensional porous structure (Fig. 4c). Intermolecular Se···Se interactions ($d_{Se\cdots Se}$ = 4.02 Å) are observed between two adjacent belts and likely contributing to the aggregates. Therefore, the belt-shaped structure of **1a** clearly implies its useful application in host-guest complexation study *vide infra*.

SCXRD analysis revealed that **1b** is a Möbius strip-shaped cage which is isomeric to **1a** as proposed by NMR and MS analysis (see Supporting information for details). As displayed in Fig. 5, one of the two DB24C8 moieties of **1b** twists and then connects to other non-twisted one, affords a twisted backbone for the strip (Fig. 5a). The puckering angle for both SeA moieties are determined to be 124° which is slightly smaller than those of **1a** indicates a greatly squeezed cavity of **1b** (Fig. 5b). Indeed, this can be further confirmed by observation of no solvent filling up its cavity while an acetonitrile and a water occupied that of the thianthrene-bridged cage [30]. Such reduced room space could hamper using **1b** as a supramolecular host. Möbius strips are chiral and can be presented as ***P*** or ***M*** enantiomers [20–23]. Accordingly, a pair of racemic cages are observed in each unit cell of the crystal from the unresolved mixture (Fig. 5c). Further packing of pairs of enantiomers along *a* and *b* axis results in the centrosymmetric structure with a non-polar space group of $P\bar{1}$ (Fig. 5d). Attempts to chiral resolution of **1b** *via* HPLC with chiral stationary phase have not meet success yet. Nonetheless, **1b** is the first example of a molecular Möbius strip-shaped cage with selenium incorporated to date.

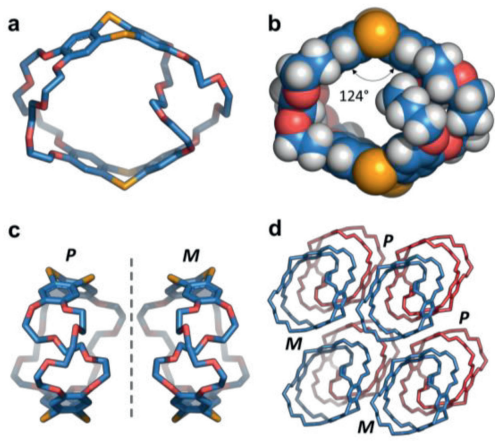

Fig. 5. Crystal structures of **1b**. Hydrogen bonds are highlighted in gray dash lines. Color code: S = Orange, O = red, N = deep blue, C = light blue and gray, Cl = green, H = white.

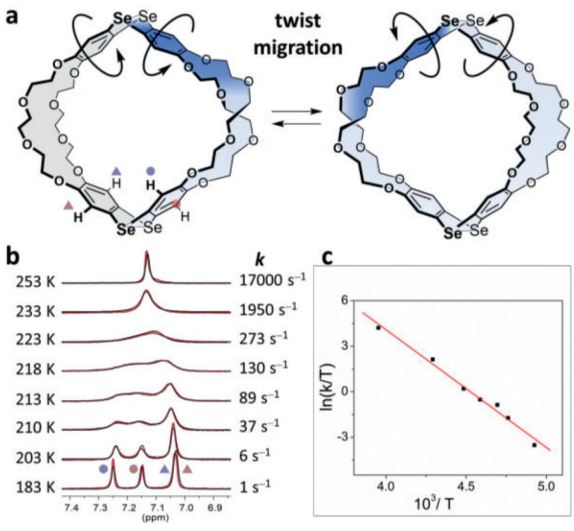

Fig. 6. (a) Schematic representation of twist migration in **1b**. (b) VT ^{1}H NMR (400 MHz, CD_2Cl_2) spectra (red trace) and simulation (black trace) with exchanging rates. (c) Eyring plot obtained from (b).

Möbius strips are known for twist migration dynamics [26,30], *i.e.* structural interconversion between the twisted and non-twisted halves of their backbones (Fig. 6a). As exemplified by an analogous thianthrene strip, the dynamic motion can be fast and associated with an energy barrier of 7.5 kcal/mol at 298 K [30]. To probe how the selenanthrene joint can influence on the migration behavior, **1b** was then subjected to variable-temperature (VT) ^{1}H NMR measurement (Fig. 6 and Fig. S3 in Supporting information). Upon cooling, the singlet resonance peak at 7.17 ppm for protons of SeA moieties gradually broadens and eventually splits into two sets of signals owing to the non-symmetrical structure of its limited conformation (Fig. 6b). The unidentical conformations of the two lateral crown ethers de-symmetrizes each SeA unit into two different benzo moieties (circle and triangle labels in Fig. 6a). The bent structure of SeA further distinguishes the two *para*-positioned protons (red and blue labels in Fig. 6a). Comparing with the coalescence temperature (T_c) of a TA-bridged strip (206 K), the higher T_c of 223 K for **1b** indicates an increased barrier for migration to occur in the SeA-bridged strip. To prove this, the VT ^{1}H NMR spectra were further simulated with different exchange rates to obtain an Eyring plot (Fig. 6c). By fitting the plot with a first-order kinetics, an activation energy barrier of 8.6 kcal/mol at 298 K was extrapolated for the twist migration to occur in **1b**. The larger barrier for **1b** to transit could be attributed to its bulker size due to selenium atoms. Thus, the incorporation of selenanthrene into a Möbius strip can slow down the twist migration.

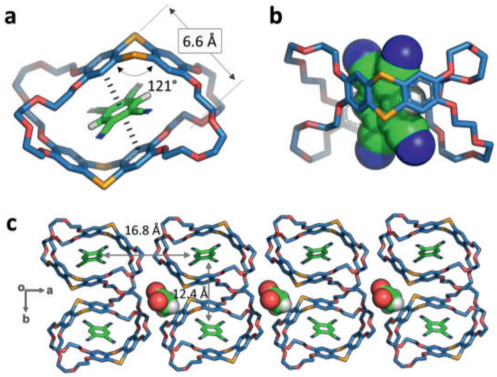

Fig. 7. Crystal structures of inclusion complex **1a**·TCNB. Hydrogen bonds and π–π interactions are highlighted in dash lines. Color code: Se = orange, O = red, C = light blue and green, N = deep blue, F = purple, H = white.

As aforementioned, the intrinsic cavity of both **1a** and **1b** implies their potential applications as supramolecular hosts. Moreover, owing to the electron-rich nature of SeA, donor-acceptor complexes have been previously reported between a tetramethoxy SeA and electron-deficient guests [36]. Accordingly, host-guest complexation studies of both cages toward a series of cyano compounds (Fig. 2b), 1,2,4,5-tetracyanobenzene (TCNB), 7,7,8,8-tetracyanoquinodimethane (TCNQ), and 2,3,5,6-tetrafluoro-7,7,8,8-tetracyanoquinodimethane (TCNQF), were subsequently evaluated by ^{1}H NMR and SCXRD analyses (see Supporting information for details). The proton NMR spectrum of an equimolar solution of **1a** and TCNB in deuterated chloroform displayed a upfield chemical shift change from 8.24 ppm to 8.14 ppm for protons of TCNB, suggested possible π-π stacking interactions between the belt and TCNB (Fig. S4 in Supporting information). Non-linear curve fitting the NMR titration data afforded a binding constant (K_a) of 31 L/mol for the complex of **1a**·TCNB (Fig. S5 in Supporting information).

Suitable single crystals of **1a**·TCNB were successfully obtained and analyzed by SCXRD (Table S4 in Supporting information). As shown in Fig. 7a, a molecule of TCNB is included in the cavity of **1a** with π-π stacking to both SeA moieties, forming a taco-like complex. To bind the flat guest tightly, **1a** has adaptively adjusted its conformation by folding both SeA units to a smaller angle (121°) and reducing the face-to-face distance of the two parallel benzoids (6.6 Å). Such an adaptive structural transformation has also resulted in a [2]pseudorotaxane structure for **1a**·TCNB (Fig. 7b). The cage **1a** stacks along the *c* crystal coordinate axis to yield one-dimensional channels which can further pack and expand into a three-dimensional (3D) porous structure (Fig. 7c). TCNB resides in the channels and forms ordered 3D arrays with separations of 16.8 and 12.4 Å along *a* and *b* axis, respectively. Smaller channels are also resulted by the packing of four adjacent cages and filled up with acetic acids.

A very similar binding behavior with a weaker binding affinity (K_a = 10 L/mol) has been observed for **1a** to interact with TCNQ in solution as determined by ^{1}H NMR study (Figs. S6 and S7 in Supporting information). SCXRD analysis (Table S5 in Supporting information) revealed an analogous [2]pseudorotaxane structure for the complex of **1a**·TCNQ (Figs. 8a-c). To fit the flat TCNQ in the cavity, **1a** has adaptively adjusted its conformation by folding both SeA units to an even smaller angle of 119°. A slightly larger face-to-face separation (6.9 Å) of the two parallel benzoids are observed for the distorted cage. π-π Stackings (d = 3.29 Å) along *b* axis are

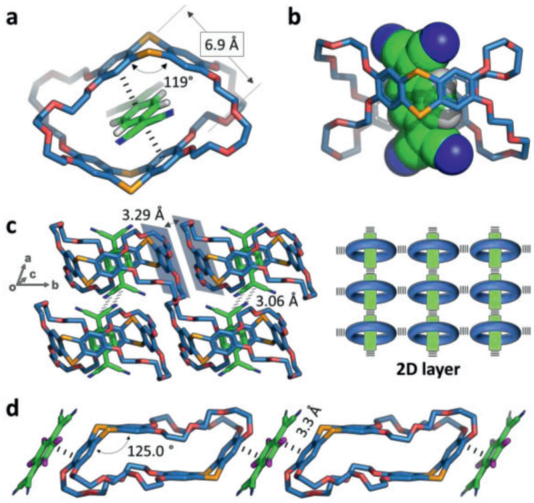

Fig. 8. Crystal structures of complexes of **1a**·TCNQ (a-c) and **1a**·TCNQF (d). Hydrogen bonds and π–π interactions are highlighted in dash lines. Color code: Se = orange, O = red, C = light blue and green, N = deep blue, F = purple, H = white.

determined for the adjacent cages. Interestingly, TCNQs in close proximity can interact with each other *via* dipole-dipole interactions (Fig. 8c). A 2D layered polyrotaxane grid is finally formed when further expand the packing structure. However, comparing with the other two guests, negligible evidence for complexation has been observed when the more electron-deficient but bulkier TCNQF was employed in NMR investigation. This result was further supported by the solid-state structure of a co-crystallized sample from an equimolar solution of **1a** and TCNQF (Fig. 8d) (Table S6 in Supporting information). The rhombus cavity of **1a** is now deformed and squeezed to a parallelepiped. Instead of forming a discrete 1:1 inclusion complex, each TCNQF π-stacks with two parallelepipeds to afford a supramolecular polymer. Conversely, no detectable evidences for host-guest complexation of Möbius strip-shaped **1b** with these guests have be observed.

To conclude, we have prepared a pair of selenanthrene-bridged molecular cages by a facile one-step cyclization reaction. The tube-shaped cage has an intrinsic cavity which can adaptively bind a series of electron-deficient guests as evidenced by NMR and single crystallography. The other product was confirmed to be a Möbius strip-shaped cage which exhibits slower twist-migration dynamics than that of a thianthrene counterpart, proving the success of structure and property regulation by incorporating selenanthrenes into molecular cages.

Declaration of competing interest

The authors declare that they have no known competing financial interests or personal relationships that could have appeared to influence the work reported in this paper.

Acknowledgments

We are grateful to National Natural Science Foundation of China (Nos. 21971268, 22171295), the Program for Guangdong Introducing Innovative and Entrepreneurial Teams (No. 2017ZT07C069), Pearl River Talent Program (No. 2017GC010623), and the Starry Night Science Fund of Zhejiang University Shanghai Institute for Advanced Study (No. SN-ZJU-SIAS-006) for financial support.

Supplementary materials

Supplementary material associated with this article can be found, in the online version, at doi:10.1016/j.cclet.2023.108179.

References

[1] Q.H. Guo, Y. Qiu, M.X. Wang, et al., Nat. Chem. 13 (2021) 402–419.
[2] S. Lei, H. Cong, Chin. Chem. Lett. 33 (2022) 1493–1496.
[3] H. Feng, Y. Chen, R. Wang, et al., Chin. Chem. Lett. 34 (2023) 108038.
[4] D. Eisenberg, R. Shenhar, M. Rabinovitz, Chem. Soc. Rev. 39 (2010) 2879–2890.
[5] L. Zhu, W. Zeng, M. Li, et al., Chin. Chem. Lett. 33 (2022) 229–233.
[6] G. Huang, W. Liu, A. Valkonen, et al., Chin. Chem. Lett. 29 (2018) 91–94.
[7] Y. Han, Z. Meng, Y.X. Ma, et al., Acc. Chem. Res. 47 (2014) 2026–2040.
[8] T. Feng, X. Li, J. Wu, et al., Chin. Chem. Lett. 31 (2022) 95–98.
[9] J. Pan, W. Lin, F. Bao, et al., Chin. Chem. Lett. 34 (2023) 107519.
[10] T.H. Shi, M.X. Wang, CCS Chem. 3 (2020) 916–931.
[11] Y. He, X. Yang, M. Qi, et al., Chin. Chem. Lett. 32 (2021) 2043–2046.
[12] Y. Xiong, C. Huang, H. Liu, et al., Chin. Chem. Lett. 32 (2021) 3522–3525.
[13] H. Kim, Y. Kim, M. Yoon, et al., J. Am. Chem. Soc. 132 (2010) 12200–12202.
[14] D.W. Zhang, W.K. Wang, Z.T. Li, Chem. Rec. 15 (2015) 233–251.
[15] M.A. Majewski, Y. Hong, T. Lis, et al., Angew. Chem. Int. Ed. 55 (2016) 14072–14076.
[16] R. Ning, H. Zhou, S.X. Nie, et al., Angew. Chem. Int. Ed. 59 (2020) 10894–10898.
[17] D. Kauerhof, J. Niemeyer, ChemPlusChem 85 (2020) 889–899.
[18] F.E. Golling, M. Quernheim, M. Wagner, et al., Angew. Chem. Int. Ed. 53 (2014) 1525–1528.
[19] S. Hitosugi, T. Yamasaki, H. Isobe, J. Am. Chem. Soc. 134 (2012) 12442–12445.
[20] R. Herges, Chem. Rev. 106 (2006) 4820–4842.
[21] S. Nishigaki, Y. Shibata, A. Nakajima, et al., J. Am. Chem. Soc. 141 (2019) 14955–14960.
[22] Y. Segawa, T. Watanabe, K. Yamanoue, et al., Nat. Synth. 1 (2022) 535–541.
[23] B. Yao, X. Liu, T. Guo, et al., Org. Chem. Front. 9 (2022) 4171–4177.
[24] D.M. Walba, R.M. Richards, R.C. Haltiwanger, J. Am. Chem. Soc. 104 (1982) 3219–3221.
[25] J.F. Ayme, J.E. Beves, C.J. Campbell, et al., Chem. Soc. Rev. 42 (2013) 1700–1712.
[26] S. Wang, J. Yuan, J. Xie, et al., Angew. Chem. Int. Ed. 60 (2021) 18443–18447.
[27] J. Xie, X. Li, S. Wang, et al., Nat. Commun. 11 (2020) 3348.
[28] J. Xie, X. Li, Z. Du, et al., CCS Chem. 5 (2023) 958–970.
[29] J. Yuan, W. Lv, A. Li, et al., Chem. Commun. 57 (2021) 12848–12851.
[30] J. Yuan, Y. Song, X. Li, et al., Org. Lett. 23 (2021) 9554–9558.
[31] S. Kim, Y. Kwon, J.P. Lee, et al., J. Mol. Struct. 655 (2003) 451–458.
[32] M.F. Peintinger, J. Beck, T. Bredow, Phys. Chem. Chem. Phys. 15 (2013) 18702–18709.
[33] A. Panda, S.C. Menon, H.B. Singh, et al., Eur. J. Inorg. Chem. (2005) 1114–1126.
[34] S. Ji, H.E. Mard, M. Smet, et al., Sci. China Chem. 60 (2017) 1191–1196.
[35] J. Shang, B. Li, X. Shen, et al., J. Org. Chem. 86 (2021) 1430–1436.
[36] H. Bock, A. Rauschenbach, C. Nather, et al., Phosphorus Sulfur 115 (1996) 51–83.